# *K*-Shell Photoabsorption Edge of Strongly Coupled Matter Driven by Laser-Converted Radiation

Yang Zhao (赵阳), Jiamin Yang (杨家敏),* Jiyan Zhang (张继彦), Guohong Yang (杨国洪), Minxi Wei (韦敏习), Gang Xiong (熊刚), Tianming Song (宋天明), Zhiyu Zhang (张志宇), Lihua Bao (鲍利华), Bo Deng (邓博), Yukun Li (黎宇坤), Xiaoan He (何小安), Chaoguang Li (李朝光), Yu Mei (梅雨), Ruizhen Yu (于瑞珍), Shaoen Jiang (江少恩), Shenye Liu (刘慎业), Yongkun Ding (丁永坤), and Baohan Zhang (张保汉)

*Research Center of Laser Fusion, China Academy of Engineering Physics, P. O. Box 919-986, Mianyang 621900, People's Republic of China*

(Received 8 July 2013; published 7 October 2013)

The first observation of the *K*-shell photoabsorption edge of strongly coupled matter with an ion-ion coupling parameter of about 65 generated by intense x-ray radiation-driven shocks is reported. The soft x-ray radiation generated by laser interaction with a "dog bone" high-*Z* hohlraum is used to ablate two thick CH layers, which cover a KCl sample, to create symmetrical inward shocks. While the two shocks impact at the central KCl sample, a highly compressed KCl is obtained with a density of 3–5 times solid density and a temperature of about 2–4 eV. The photoabsorption spectra of chlorine near the *K*-shell edge are measured with a crystal spectrometer using a short x-ray backlighter. The redshift of the *K* edge up to 11.7 eV and broadening of 15.2 eV are obtained for the maximum compression. A comparison of the measured redshifts and broadenings with dense plasma calculations are made, and it indicates potential improvements in the theoretical description.

DOI: 10.1103/PhysRevLett.111.155003 PACS numbers: 52.50.Lp, 32.30.Rj, 52.25.Os

Warm dense matter (WDM) that is near or above the solid density and by a temperature of up to to 100 eV exists in large varieties of systems such as astrophysics objects and an imploded capsule of inertial confinement fusion. Over the past decades, there has been increased interest in understanding the properties of WDM [1–3], and great progress on both theoretical and experimental studies of the properties has been made. However, a challenge of these studies is to understand the properties of highly compressed WDM with a large ion-ion coupling parameter, as required in planetary interiors [4] and inertial confinement fusion [5]. Thus, it is crucial to create in a laboratory strongly coupled matter with high density and to take characteristic measurements of the dense matter. Different from the standard property measurements, including the equation of state along the Hugoniot [6], reflectivity, and conductivity [7], x-ray absorption can provide direct information about the density, temperature, electronic, and ionic structures of dense matter. Therefore, obtaining detailed measurements of x-ray absorption spectra, especially near the absorption edge of highly compressed matter, is very appealing.

With the advent of the high-power laser, laser-driven shocks have been used to generate high-compression WDM with pressure over 10 Mbar [8], and a few experiments on the x-ray absorption of warm dense matter have been carried out in recent years. Bradley [9] made the first measurement of the shift in position of the *K*-shell absorption edge in a laser-heated and -shocked KCl material to demonstrate the pressure ionization that was due to high density. In this experiment, the KCl sample was radiatively preheated and then shock compressed to a state of about 3 times solid density (6.2 g/cm$^3$ and 19 eV). (As is well known, the maximum compression ratio that can be achieved with a single shock wave is about 4 [10]). In order to take x-ray absorption spectrum measurements under higher compression, following Bradley's experiment great efforts were made on the aluminum sample to increase the density. In Hall's experiment, laser-driven colliding shocks were used to compress an aluminum sample [11]. Short-range order within the compressed plasma has been observed by means of the extended x-ray absorption fine-structure spectrum of the aluminum *K* absorption edge. Benuzzi-Mounaix put a diamond layer on the back of an aluminum sample as a tamper to form reshocks in the sample as the laser-driven shock reached the Al-diamond interface [12]. Reshocked aluminum conditions up to 3 times solid density and at temperatures around 8 eV have been obtained. The electronic structure evolution of this highly compressed aluminum has been investigated using time-resolved *K*-edge x-ray absorption spectroscopy. Regan adopted temporally shaped laser ablation to compress an aluminum sample [13]. A highly compressed Fermi-degenerated plasma has been created. A density of about 11 g/cm$^3$ ($\sim 4\rho_0$) and a temperature of 20 eV for aluminum plasma have been obtained, and the ion-ion coupling parameter reached about 10. However, in almost all of the experiments, the laser irradiated the tamped target directly to compress the sample. Hard x-ray radiation and energetic electrons from the corona of laser-produced plasmas, which increased with the laser intensity, preheated the sample before the shock-wave

 

compression occurred and reduced the compressibility of the sample [14]. Therefore, until now, the density of the compressed sample was not over 4 times that of solid density in these x-ray absorption spectrum experiments.

In this Letter, the measurements of the $K$ edge of Fermi-degenerated KCl are the first ones obtained at densities up to 5 times solid density with a low temperature around 4 eV. For the generation of this state, unexplored up to now, near-Plank x-ray radiation-driven shocks instead of laser-driven shocks were adopted to take the colliding shock compression. By using a "dog bone" hohlraum, the sample was shielded from the laser-hitting point to stop the $M$-band x ray and energetic electrons from the corona preheating the sample, and thus, the compressibility was enhanced. Using a short laser interaction with a bismuth target as a backlighter, the $K$-edge variations of the KCl sample under the colliding shock conditions were measured to study the electronic structure in comparison with a plasma model.

The experiment was performed at the Shenguang-II Laser facility [15,16]. A schematic of the experimental setup is shown in Fig. 1(a). A dog bone gold hohlraum was used as an x-ray converter. Eight frequency-tripled laser beams ($\lambda = 0.35$ $\mu$m, 260 J in 1 ns for each laser beam) were injected into the hohlraum from two laser entrance holes (LEHs). The laser lights (hereafter referred to as the "heating laser") were effectively converted into the near-Planck x-ray radiation. A half-sample sandwich target located in the center of the cylindrical part was used to accomplish simultaneous measurements of the backlighting spectrum and the absorption spectrum in one shot, as shown in Fig. 1(b). The sample was composed of a central KCl sample layer with a thickness of 5 $\mu$m and a density of 2.0 g/cm$^3$ and two plastic ablators on both sides. The thickness and density of the plastic ablator was 38 $\mu$m and 1.0 g/cm$^3$, respectively.

The near-Plank radiation ablated the CH ablators from both sides to launch symmetrical inward shocks. While the

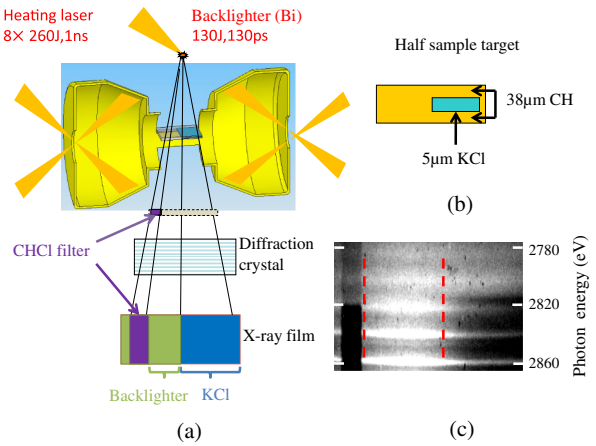


FIG. 1 (color online). (a) Schematic of the experimental setup. (b) Half-sample sandwich target. (c) Typical spectral image.

two shocks simultaneously propagated into the KCl layer and collided at the center, a high maximum compression state of the sample was created. The covered CH thickness was chosen by considering the following: First, had to be thick enough to stop the x-ray radiation from burning through the CH ablator and avoid radiative heating of the central KCl sample. Second, the time-resolving measurements required that the CH thickness fit in order to keep the KCl sample in a high-density state for a relatively long duration compared with the duration of the x-ray backlighter. Third, as the two CH layers significantly attenuated the backlighter x-ray near the absorption edge, the thickness of the CH layer also depended on the sensitivity of the crystal spectrometer and the x-ray intensity of the backlighter. Thus, the CH thickness was set at an appropriate value of 38 $\mu$m in this experiment. By using the $D$-shaped cavity, the central target was invisible to the laser-hitting point, and therefore, it stopped the $M$-band x rays from preheating and scattered laser lights ablating the sample located in the center of the dog bone gold hohlraum. Consequently, the KCl sample was compressed only by the near-Planck x-ray radiation-driven shocks without preheating.

The spectrally flat x-ray backlighting source was obtained by focusing the ninth frequency-tripled laser beam (130 J, 130 ps) onto a bismuth disk. A crystal spectrometer consisting of a Bragg Tris(hydroxymethyl) aminomethane $[HOCH_2]_3CNH_2$ plane crystal ($2d = 8.78$ Å) and an x-ray film as a recorder was used for the time- and space-resolving spectral measurement, as the x-ray backlighter was a short pulse and point x-ray source. A CHCl filter positioned at the entrance slot of the crystal spectrometer on the pure CH side of the sample was used to produce a cold Cl $K$ edge at 2821 eV on the backlighting source spectrum region and acted as a wavelength reference [17]. As shown in Figs. 1(a) and 1(c), the recorded spectrum mainly consisted of three portions along a space, including the absorption spectrum of the cold CHCl filter, the backlighting x-ray source spectrum, and the absorption spectrum of the compressed KCl sample.

A soft x-ray spectrometer was used to monitor the temporal process of the driving radiation from the LEH. The measured peak temperature of the radiation was 105 eV. A view factor analysis of the illumination in the $D$-shaped cavity showed that the peak radiation temperature of the near-Plank radiation at the sample was 90 eV, which was lower than that measured from the LEH. The modified temporal behavior of the radiation is shown in Fig. 2(a), with a peak radiation temperature at 1.05 ns after the heating laser irradiation. Then, using the modified radiation as an x-ray source, the hydrodynamic process of the CH/KCl/CH sample in the present experiment was simulated by the MULTI code [18]. This procedure was previously established by the temperature diagnostics in the Fe plasma opacity experiment [16]. In that experiment,

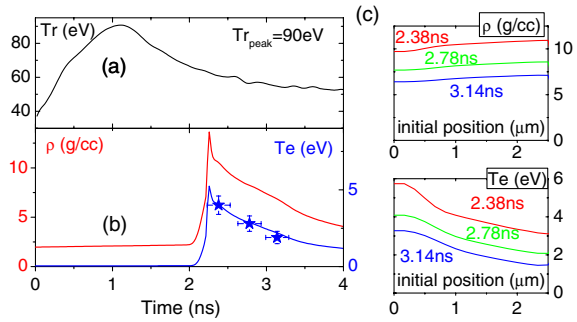


FIG. 2 (color online). (a) The modified temporal behavior of the radiation at the sample, with a peak temperature of 90 eV. (b) The simulated evolution of temperature and density of the KCl in the CH/KCl/CH multilayer foil as compressed by the near-Plank x-ray radiation-driven colliding shocks. The solid pentacles refer to the temperatures deduced from the measured $K$ edge broadening at different time delays of 2.38, 2.78, and 3.14 ns. (c) The $\rho$ and $T$ spatial profile from the center of the KCl sample to the edge at time delays.

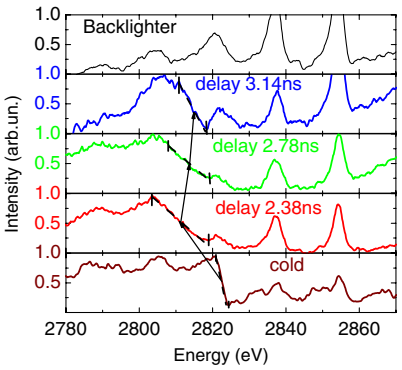


FIG. 3 (color online). Measured backlighter x-ray source spectrum and $K$-shell edge absorption spectra of the compressed KCl sample at different time delays of 2.38, 2.78, and 3.14 ns. As a comparison, the $K$-shell edge absorption spectrum for a cold KCl sample (with the eight heating laser beams off) is also presented at the bottom.

only the CH/FeAl/CH sample (instead of the present CH/KCl/CH sample) in the dog bone cavity and the temperature of the sample were measured by a crystal spectrometer. The measured temperature was in good agreement with the MULTI simulation using the modified near-Plank radiation due to the specific dog bone cavity, which confirmed the procedure. This allowed us to evaluate the density $\rho$ and the temperature $T$ of the probed KCl by coupling the modified radiation into the MULTI code. The simulated results are shown in Figs. 2(b) and 2(c). The temperature and density started to increase obviously at 2.05 ns and went to a maximum at 2.25 ns, which indicated that the radiation-driven shocks collided at the center of the KCl sample at 2.25 ns. Then, the temperature and density gradually decreased as time went on. The ninth beam was delayed to eight heating laser pulses at time delays of 2.38, 2.78, and 3.14 ns to obtain time-resolving measurements along the shock conditions. Figure 2(c) shows the spatial profile of the temperature and density of the KCl sample at the three time delays. The density of the KCl sample was almost spatially uniform and the temperature decreased gradually from the center to the border of the KCl sample.

Using the experimental setup described above, space-resolved absorption spectra were measured at the three different time delays. A typical recording of the spectral image is shown in Fig. 1(c). The three zones on the film discussed above were labeled. Reference lines of Bi at 2854.4 eV [19] and a Cl $K$ edge of the cold CHCl filter at 2821 eV [17] were used to calibrate the spectral wavelength. The spectral resolution of about 3 eV was estimated from the cold CHCl $K$-edge spectrum measurement.

Figure 3 shows the $K$-edge absorption spectra of the compressed KCl sample at the three time delays. Also presented are the spectrum of the backlighting x-ray source and the absorption spectrum of the unheated KCl sample. The shifts and broadenings of the Cl $K$-shell absorption edge for the compressed KCl sample are obvious and listed in Table I. While the shocks collided at the center of the KCl sample, the $K$ edge had a maximum redshift and width of 11.7 and 15.2 eV, respectively. Then, the shift and width decreased along the unloading process.

Recently, a simple model was proposed for high-density low-temperature WDM ($\mathrm{Te} \leq E_F/4$). In that model, $K$-edge broadening revealed the thermal broadening of the Fermi level [20]. The electron temperature could even be deduced from a simple analytical fit of the $K$-edge width by the Fermi-Dirac "vacancy" factor $[1 - f(\varepsilon)]$. Here, by the slope fit of the measured x-ray absorption $K$-edge broadening, the electron temperature was inferred to be $4.0 \pm 0.6$ eV, $2.8 \pm 0.5$ eV, and $1.9 \pm 0.4$ eV at the different time delays, as listed in Table I and presented in Fig. 2(b). It was shown that the experimental temperatures at all three time delays were consistent with the results of the simulations. The agreement confirms that the broadening of the $K$-shell absorption edge was due to the thermal depopulation of the energy levels below the Fermi level in this compressed-state region.

The $K$-edge shifts were predicted by a plasma model including three contributions as described in the previous KCl experiment [9]. The first contribution $\triangle I_k$ was the change in the average $K$-shell ionization energy of an isolated atom, and it was calculated with the flexible atomic code [21], in which the average ionization was taken from Thomas-Fermi model [22]. The second contribution $\triangle E_{cl}$ represented the continuum lowering due to the influence of the neighbors and was approximately calculated by a finite-temperature Thomas-Fermi model [23]. The third contribution $\triangle E_{\mathrm{deg}}$ represented the partial degeneracy of the free-electron states close to the ionization energy [24].

Figure 4(a) shows the three contributions and the total $K$-edge shifts along the colliding shocked conditions. The total $K$-shell edge shift mainly came from the competition between the blueshift in the edge from the ionization effect

TABLE I. The redshift and width of the $K$-absorption edge of the highly compressed KCl at different time delays and the cold KCl. The temperatures and densities were obtained from the hydrodynamic simulations, and the temperatures in the brackets were deduced from a Fermi-Dirac fit of the edge slope.

| | Cold | Delay 2.38 ns | Delay 2.78 ns | Delay 3.14 ns |
|---|---|---|---|---|
| Positions | 2821.3–2824.3 eV | 2803.5–2818.7 eV | 2807.8–2819.3 eV | 2810.4–2818.2 eV |
| Shift | 0 eV | −11.7 eV | −9.25 eV | −7.6 eV |
| Width | 3 eV | 15.2 eV | 11.5 eV | 7.8 eV |
| Te | 0 eV | 4.0 eV (4.0 ± 0.6 eV) | 2.8 eV (2.8 ± 0.5 eV) | 2.2 eV (1.9 ± 0.4 eV) |
| Density | 2.0 g/cm$^3$ | 10.5 g/cm$^3$ | 8.3 g/cm$^3$ | 6.9 g/cm$^3$ |

and the redshift due to continuum lowering, while the degenerate term was not significant in our experimental condition. In Fig. 4(b), the density uncertainties due to the probing time uncertainty, temporal and spatial profiles during the probing window, and the radiation temperature difference from shot to shot have been included in the plotted error bars. Though the experimental observation showed a general agreement with the simulated curve along the colliding shocked conditions, the experimental redshifts of the $K$-shell edge showed a slower increase with density compared with the simulated curve, which was also observed in Benuzzi-Mounaix's experiment of aluminum [12]. The discrepancy was perhaps because the average ionization degree predicted by Thomas-Fermi model was rough for this middle $Z$ element in the plasma model adopted here, and therefore the accuracy of the ionization energy shift $\triangle I_k$ and the continuum lowing $\triangle E_{cl}$ was somewhat affected.

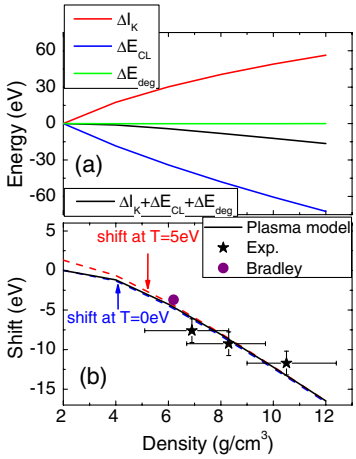


FIG. 4 (color online). (a) Calculated total shifts of the $K$-shell absorption edge and the three contributions as functions of the density of the KCl sample compressed by the radiation-driven colliding shocks using a plasma model. (b) Comparison of the experimental $K$-edge shift results (solid pentacle represents our results, purple circle represents Bradley's result) with the calculation curve along the compressed state of the KCl sample in this experiment based on the plasma model. Also presented are the calculated shifts of the Cl $K$-shell absorption edge as a function of the density for temperatures of 0 (blue dashed line) and 5 eV (red dashed line).

To isolate the density effect, Fig. 4(b) also shows the predicted total shifts of the $K$-shell absorption edge as a function of density at temperatures of 0 and 5 eV. The two curves show that the redshift increased with increasing density and weakly depended on the temperature. Therefore, the large shift obtained in our experiment indicated that high-density and low-temperature states of the compressed KCl were reached. Additionally, the redshift of 3.7 eV in Bradley's one-sided shock-compressed KCl experiment (6.2 g/cm$^3$, 19 eV) [9] is also plotted to highlight the importance of our results that lie in an extreme region unexplored up to now.

Compared with laser-driven shock compression, low preheating and colliding shocks synchronization can be easily realized using radiation-driven shocks and a symmetrical target design. The ion-ion coupling parameter $\Gamma_{ii} = (Ze)^2/dk_BT$ obtained here was around 65, while the compression ratio reached 5 times. For widely investigated warm dense aluminum using the same target design and near-Planck radiation as a driving x-ray source, the hydrodynamic simulations predicted that the density could increase up to 11 g/cm$^3$ ($\sim 4\rho_0$) with a low temperature of about 2.5 eV, which was also an unexplored state for aluminum until now.

In summary, we performed time-resolved $K$-edge absorption measurements of the KCl sample at the states created by x-ray radiation-driven shock-colliding compression. An unexplored and extreme state of the plasma with the maximum of 5 times solid density and a temperature of about 4 eV ($\Gamma_{ii} \sim 65$, with an average ionization of 4.5) were reached. This method of compression is more advantageous than laser-driven shocks for the generation of an extreme compression state at a high coupling parameter. The shifts and broadening of the $K$-shell absorption edge of the highly compressed KCl have been obtained and compared with the calculations of the plasma model. It was confirmed that the broadening of the $K$-shell absorption edge was due to the thermal depopulation of the energy levels below the Fermi level in the compressed-state region. The shift of the $K$-shell absorption edge increased with increasing density but weakly depended on the temperature. The experimental shifts were in general agreement with the calculations of the plasma model along the colliding shocked conditions. But more improvements are desired to describe in detail the variation of the

*K*-edge shifts as a function of the density. This work might extend to the study of WDM to extreme conditions of high compression.

The authors would like to thank the target fabrication and the laser operation staffs for their cooperation. This work is supported by the National Nature Science Fund of China (Grant No. 11304292), the Foundation of China Academy of Engineering Physics (Grant No. 2011A0102005), and the Foundation of Science and Technology on Plasma Physics Laboratory (Grant No. 9140C680203110C6804).

*yjm70018@sina.cn

[1] G. W. Collins *et al.*, Science **281**, 1178 (1998).
[2] M. D. Knudson, D. L. Hanson, J. E. Bailey, C. A. Hall, and J. R. Asay, Phys. Rev. Lett. **87**, 225501 (2001).
[3] J. Eggert, S. Brygoo, P. Loubeyre, R. S. McWilliams, P. M. Celliers, D. G. Hicks, T. R. Boehly, R. Jeanloz, and G. W. Collins, Phys. Rev. Lett. **100**, 124503 (2008).
[4] D. Saumon and G. Chabrier, Phys. Rev. A **44**, 5122 (1991).
[5] J. D. Lindl, P. Amendt, R. L. Berger, S. G. Glendinning, S. H. Glenzer, S. W. Haan, R. L. Kauffman, O. L. Landen, and L. J. Suter, Phys. Plasmas **11**, 339 (2004).
[6] M. Koenig, B. Faral, J. M. Boudenne, D. Batani, A. Benuzzi, S. Bossi, C. Rémond, J. P. Perrine, M. Temporal, and S. Atzeni, Phys. Rev. Lett. **74**, 2260 (1995).
[7] P. M. Celliers *et al.*, Phys. Plasmas **11**, L41 (2004).
[8] M. D. Knudson and M. P. Desjarlais, Phys. Rev. Lett. **103**, 225501 (2009).
[9] D. K. Bradley, J. Kilkenny, S. J. Rose, and J. D. Hares, Phys. Rev. Lett. **59**, 2995 (1987).
[10] R. P. Drake, *High Energy Density Physics: Fundamentals, Inertial Fusion, and Experimental Astrophysics, Shock Wave and High Pressure Phenomena.* (Springer, New York, 2006).
[11] T. A. Hall, A. Djaoui, R. W. Eason, C. L. Jackson, B. Shiwai, S. L. Rose, A. Cole, and P. Apte, Phys. Rev. Lett. **60**, 2034 (1988).
[12] A. Benuzzi-Mounaix *et al.*, Phys. Rev. Lett. **107**, 165006 (2011).
[13] S. P. Regan *et al.*, High Energy Density Phys. **7**, 259 (2011).
[14] H. Sawada *et al.*, Phys. Plasmas **16**, 052702 (2009).
[15] Y. Zhao, J. Yang, J. Zhang, J. Liu, X. Yuan, and F. Jin, Rev. Sci. Instrum. **80**, 043505 (2009).
[16] J. Y. Zhang *et al.*, Phys. Plasmas **19**, 113302 (2012).
[17] D. Riley, O. Willi, S. J. Rose, and T. Afshar-Rad, Europhys. Lett. **10**, 135 (1989).
[18] R. Ramis, R. Schmalz, and J. Meyer-Ter-Vehn, Comput. Phys. Commun. **49**, 475 (1988).
[19] S. Elliott, P. Beiersdorfer, and J. Nilsen, Phys. Rev. A **47**, 1403 (1993).
[20] F. Dorchies, in International Workshop on Warm Dense Matter, Pacific Grove, CA, USA, 2011.
[21] M. F. Gu, Astrophys. J. **582**, 1241 (2003).
[22] D. Salzmann, *Atomic Physics in Hot Plasma* (Oxford University Press, New York, 1998).
[23] J. C. Stewart, and K. D. Pyatt, Jr., Astrophys. J. **144**, 1203 (1966).
[24] J. P. Cox, *Principles of Stellar Structure* (Gordon and Breach, New York, 1968).